euronoise

Vibroacoustic Simulation of Partly Immersed Bodies by a Coupled Fast BE-FE Approach

Dominik Brunner[a], Michael Junge[a], Christian Cabos[b] and Lothar Gaul[a]

[a]Institute of Applied and Experimental Mechanics, University of Stuttgart, Pfaffenwaldring 9, 70550 Stuttgart, Germany
[b]Germanischer Lloyd, Vorsetzen 35, 20459 Hamburg, Germany
brunner@iam.uni-stuttgart.de

Simulation of vibro-acoustic behavior of submerged bodies necessitates dealing with fluid-structure coupled problems. Due to the high density of the fluid, the feedback of the acoustic pressure onto the structure cannot be neglected and a fully coupled system must be investigated. The boundary element method (BEM) is well suited for simulating the sound propagation in an unbounded exterior acoustic fluid domain. Here, the fast multipole method (FMM) is applied to overcome the known bottleneck of classical BE-methods. In the case of partly immersed bodies, Dirichlet boundary conditions on the fluid surface have to be incorporated additionally. This is done by applying a half-space formulation. The extension of the FMM to this scenario is discussed. The finite element method (FEM) is used for the structural part. The commercial finite element package ANSYS is applied for setting up the mass and stiffness matrices. A preconditioned iterative solver is employed and the numerical efficiency is discussed. The applicability of the coupling scheme is demonstrated using a realistic model problem.

1 Introduction

For the simulation of the vibrations of ship-like structures, the surrounding water has to be taken into consideration. In case of surface ships, the fluid domain Ω_a forms a semi-infinite half-space (cf. Fig. 1). Problems with infinite domains can efficiently be treated with the BEM, since only the boundary of an investigated structure within this domain has to be discretized. The free field condition, also known as Sommerfeld condition, is automatically fulfilled by the fundamental solution. This procedure can also be applied to half-space problems. Here, a modified fundamental solution is chosen, which satisfies the boundary condition on the half-space plane [1]. For a free water surface, a Dirichlet boundary condition with vanishing pressure has to be applied. Unfortunately, the naive use of the BEM results in fully populated matrices with an expense of order $\mathcal{O}(N^2)$ for a problem with N degrees of freedom. If a direct solver is applied, one even has an expense of order $\mathcal{O}(N^3)$. To overcome this drawback, the FMM is applied in this paper, which has an almost linear expense of order $\mathcal{O}(N \log^2 N)$. The treatment of half-space problems involves some modifications of the usually applied multipole cycle. Nevertheless, the modified fundamental solution is incorporated in a very efficient way. To take full advantage of the FMM, which is capable to provide a matrix-vector product, one favorably applies an iterative solver.

For the structural part Ω_s, the FEM is the favorite choice. The discretization results in sparse matrices. Typically, ship-like structures are modeled with shell elements. The resulting matrices have a very poor condition number, which makes the use of direct solvers preferable to the use of iterative solvers.

The two domains are coupled on the fluid-structure interface Γ_I [5]. An efficient way to solve the coupled system is the use of a Schur complement formulation [6]. Thus, an iterative solver is applied for the outer loop with the BE matrices and the inverse of the BE matrix within the Schur complement is computed by a direct solver.

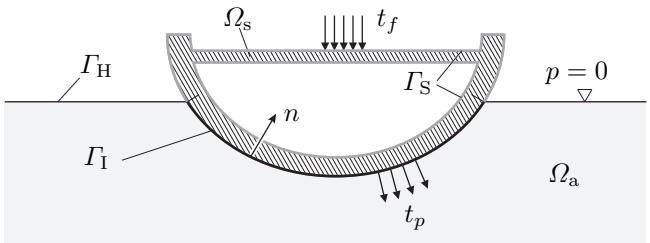

Figure 1: The investigated half-space problem consists of a structural domain Ω_s and an exterior acoustic domain Ω_a which are coupled on Γ_I.

The paper is organized as follows: First, the BE representation of the half-space problem is discussed. Then, the efficient implementation by the multilevel FMM is presented. After this, the application of the FEM to the structural part is outlined and the coupled system is set up. At the end, a realistic container-vessel is investigated with the proposed approach.

2 Fast BEM for the Fluid Domain

As governing equation for the acoustic pressure p of the fluid domain, the linear time-harmonic Helmholtz equation

$$\Delta p(x) + \kappa^2 \, p(x) = 0 \,, \qquad x \in \Omega_\mathrm{a} \tag{1}$$

is chosen, where Δ denotes the Laplacian. The circular wavenumber is given by $\kappa = \omega/c$, with the angular frequency ω and the speed of sound c. Throughout this paper, the time harmonic behavior $\mathrm{e}^{-\mathrm{i}\omega t}$ is applied. In the following, a boundary integral representation for the half-space problem is discussed.

2.1 Boundary Integral Equations

Starting point is the weak form of the Helmholtz equation, which is obtained by weighting with a fundamental solution $P(x, y)$. For the investigated half-space problem, the modified fundamental solution [1]

$$P(x,y) = \frac{1}{4\,\pi} \frac{\mathrm{e}^{\mathrm{i}\,\kappa\,|x-y|}}{|x-y|} - \frac{1}{4\,\pi} \frac{\mathrm{e}^{\mathrm{i}\,\kappa\,|\tilde{x}-y|}}{|\tilde{x}-y|} \,, \tag{2}$$

is applied, where the point x is mirrored on the half-space plane to yield $\tilde{x}$. Applying Green's second theorem yields the representation formula

$$p(x) = -\int_{\Gamma_\mathrm{I}} P(x,y) \, \frac{\partial p(y)}{\partial n_y} \mathrm{d}s_y + \int_{\Gamma_\mathrm{I}} \frac{\partial P(x,y)}{\partial n_y} \, p(y) \, \mathrm{d}s_y \,, \tag{3}$$

which is valid for an arbitrary point x within Ω_a. Obviously, the infinite half-space plane does not have to be discretized at all. This is because of the special choice of the fundamental solution. Moving the point x onto the smooth boundary by a limit process yields the two

boundary integral equations

$$\frac{1}{2}p(x) = \underbrace{\int_{\Gamma_\mathrm{I}} P(x,y)\frac{\partial p(y)}{\partial n_y}\,\mathrm{d}s_y}_{(Vq)(x)} - \underbrace{\int_{\Gamma_\mathrm{I}} \frac{\partial P(x,y)}{\partial n_y} p(y)\,\mathrm{d}s_y}_{(Kp)(x)}, \tag{4}$$

$$\frac{1}{2}q(x) = \underbrace{\int_{\Gamma_\mathrm{I}} \frac{\partial P(x,y)}{\partial n_x}\frac{\partial p(y)}{\partial n_y}\,\mathrm{d}s_y}_{(K'q)(x)} - \underbrace{\int_{\Gamma_\mathrm{I}} \frac{\partial^2 P(x,y)}{\partial n_x \partial n_y} p(y)\,\mathrm{d}s_y}_{-(Dp)(x)}, \tag{5}$$

with the single layer potential V, the double layer potential K, its adjoint K' and the hypersingular operator D. Here, the acoustic flux $q(x) = {}^{\partial p(x)}/_{\partial n_x}$ is introduced. The two integral equations (4) and (5) are weighted with linear functions to obtain a Galerkin formulation. Now, the boundary Γ_I is discretized with triangular elements. Piecewise linear basis functions $\varphi_i(x)$ are applied for the interpolation of p and discontinuous ones for the acoustic flux q. To overcome the well-known non-uniqueness problems, the Burton-Miller approach is applied, which is a linear combination of both integral equations. The resulting system of equations reads

$$\underbrace{\left(\frac{1}{2}\boldsymbol{M} + \boldsymbol{K} + \frac{\mathrm{i}}{\kappa}\boldsymbol{D}\right)}_{\boldsymbol{K}_\mathbf{BE}}\boldsymbol{p} - \underbrace{\left(\boldsymbol{V} + \frac{\mathrm{i}}{2\kappa}\boldsymbol{M}' - \frac{\mathrm{i}}{\kappa}\boldsymbol{K}'\right)}_{\boldsymbol{C}_\mathbf{BE}}\boldsymbol{q} = 0\,, \tag{6}$$

where $\boldsymbol{M}$, $\boldsymbol{K}$, $\boldsymbol{D}$ and $\boldsymbol{V}$ represent the Galerkin matrices corresponding to the operators in (4) and (5). For coupling with the FEM, the acoustic flux on an BE element m needs to be expressed by the structural displacements of the adjacent nodes k. Using Euler's equation, this is done by

$$q_m = \frac{1}{3}\varrho_\mathrm{f}\omega^2 \sum_{k\in m} u^k_{n^m}\,, \tag{7}$$

with the fluid density ϱ_f and the nodal displacement $\boldsymbol{u}^k_{n^m}$ at node k in normal direction of the element m. This is a simple averaging which turned out to be suitable for engineering applications [6]. In matrix notation, (7) is written as

$$\boldsymbol{q} = \boldsymbol{T}_q\boldsymbol{u}\,, \tag{8}$$

where $\boldsymbol{u}$ is a vector with the displacements and rotations of the strucural nodes. Matrix $\boldsymbol{T}_q$ is sparse and filled with zeros for degrees of freedom which are not in contact with the fluid.

To avoid setting up the fully populated matrices $\boldsymbol{K}_\mathbf{BE}$ and $\boldsymbol{C}_\mathbf{BE}$, the FMM is applied in the following.

2.2 Cluster Tree of the Half-Space FMM

The second term in the fundamental solution (2) accounts for the point $\tilde{x}$, which is obtained by mirroring x on the half-space plane. Thus, an efficient strategy for the FMM is to simply mirror the whole geometry with its elements and nodes. This way, the standard kernels and the multipole series expansion is still applicable. The first step is the introduction of a hierarchical cluster tree, which is built by bisectioning (cf. Fig. 2). The root cluster contains all elements. Every father cluster on level ℓ is split into two son clusters on level ℓ+1. Clusters which do not have any sons are called leaf-clusters.

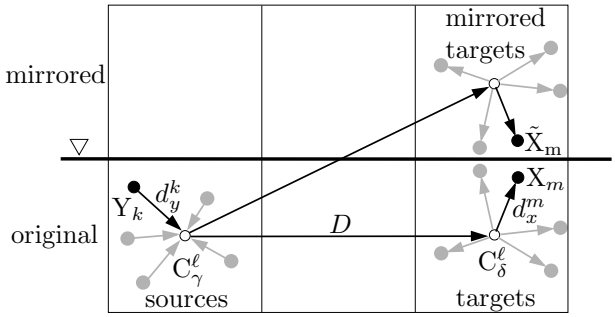

Figure 2: Clustering of the sources and the targets.

A cluster c_γ^ℓ on level ℓ is said to be in the near-field of c_δ^ℓ if the condition

$$\mathrm{dist}(\mathrm{C}_\gamma^\ell, \mathrm{C}_\delta^\ell) \le c_d \max(d_\gamma^\ell, d_\delta^\ell) \tag{9}$$

is satisfied, where d_γ^ℓ is the cluster diameter of c_γ^ℓ. Please note, that clusters in the mirrored part are always target-clusters but never source-clusters. Since most of the the mirrored clusters are far away from the half-space plane, most of the interaction is in the far-field part, giving a good far-field compression. Clusters whose father clusters are in each others near-field but themselves are not in the near-field of each other, form the so-called interaction list.

2.3 Near-Field of the FMM

The multipole expansion is only valid for the far-field, where the points are well-separated. The near-field has to be integrated in the classical way. Due to the mirror technique, the already existing integration routines are applied. Only some additional calls are necessary for elements in mirrored target clusters, which are close to the half-space plane and fulfill the near-field condition (9) . The result of the integration has to be subtracted from the entries at the corresponding non-mirrored node locations of the sparse near-field matrix. Thus the overall size and memory consumption is not influenced by the mirror technique.

2.4 Far-Field of the FMM

For the introduced operators, one has to evaluate potentials of the type

$$\Phi(x_m) = \sum_{k=1}^{A} \frac{\mathrm{e}^{\,\mathrm{i}\kappa|x_m - y_k|}}{|x_m - y_k|} q_k, \tag{10}$$

where q_k denotes the source strengths of A sources and $|x_m - y_k|$ is the distance between the field and load point. Introducing the translation operator

$$M_L(s,D) = \sum_{l=0}^{L} (2l+1)\mathrm{i}^l h_l^{(1)}(\kappa|D|) P_l(s\cdot\hat{D})\,, \tag{11}$$

with the Hankel functions h_l and the Legendre polynoms P_l, the original potential (10) can be expressed in

the form

$$\Phi(x_m) = \frac{\mathrm{i}\kappa}{4\pi} \int_{\mathbb{S}^2} \mathrm{e}^{\mathrm{i}\kappa\, d_x^m \cdot s} M_L(s,D) \underbrace{\sum_{k=1}^{A} \mathrm{e}^{\mathrm{i}\kappa\, d_y^k \cdot s} q_k}_{F(s)} \,\mathrm{d}s\,, \tag{12}$$

where d_x^m, D and d_y^k are visualized in Fig. 2. The choice of L in (11), which is called the expansion length, has a significant influence on the accuracy and the performance of the multipole algorithm. Proper choice helps to achieve a desired accuracy and avoids possible divergence of the series. Typically, the semi-empirical rule [3]

$$L\,(\kappa\, d_\ell) = \kappa d_\ell + c_\mathrm{e} \log\,(\kappa\, d_\ell + \pi) \tag{13}$$

is used to estimate the number of series terms on level ℓ of the cluster tree. The parameter c_e has to be chosen by the user and determines the accuracy.

The sum on the right hand side of (12) is called the far-field signature $F(s)$. It is local to the cluster with the sources q_k, since only the vector d_y^k appears. In contrast to this, the translation operator M_L only depends on the vector D between two clusters' centers. Thus, if a regular cluster grid is used, the translation operators can be re–used. Translating the far-field signature to the clusters of its interaction list using a translation operator forms the so called near-field signature $N(s)$. The solution is finally recovered by an exponential function of d_x^m and an integration over the unit sphere. The resulting FMM has a quasi linear complexity of order $\mathcal{O}(N \log^2 N)$.

The evaluation of the matrix-vector product with the FMM algorithm is similar for all operators which are needed for the coupling formulations. Only slight modifications are necessary in order to take into account the different test and shape functions. The general procedure can be summarized with the following steps:

1. Compute the near-field part by a sparse matrix–vector multiplication.
2. Evaluate the far-field signature $F(s)$ for all leaf clusters in the non-mirrored part.
3. Translate the far-field signature to all interaction cluster by means of the translation operators (11) and sum it up as the near-field signature $N(s)$ there. Mirrored clusters have to be considered in the interaction lists.
4. Shift the far-field signature to the father cluster and repeat step 3 until the interaction list is empty.
5. Go the opposite direction and shift the near-field signature $N(s)$ for the non-mirrored and mirrored clusters to the son clusters until the leaf clusters are reached.
6. Recover the solution by integration over the unit sphere and the elements. The result at a node of the mirrored part has to be subtracted from the corresponding non-mirrored entry.

There are two main advantages if the mirror technique is applied with the FMM. First, the additional expense for the near-field is small, since only a few mirrored clusters are in the near-field of a non-mirrored source cluster. Second, the standard multipole expansion can be applied. Most of the interaction to the mirrored part is on the coarser levels, which gives a good efficiency of the FMM.

3 FEM for the Structural Domain

The finite element package ANSYS is utilized to set up a linear system of equations for the structural domain Ω_s which is modeled with the elasto-dynamic field equation

$$\omega^2 \varrho_\mathrm{s}\, u(x) + \mu \Delta u(x) + (\lambda + \mu)\, \mathrm{grad}\, \mathrm{div}\, u(x) = 0\,. \tag{14}$$

The tractions t_s are prescribed on Γ_s. The resulting mass matrix $\boldsymbol{M}_\mathrm{s}$, the stiffness matrix $\boldsymbol{K}_\mathrm{s}$ and the right hand side vector $\boldsymbol{f}_\mathrm{s}$ are imported into the research code by a binary interface. Vector $\boldsymbol{f}_\mathrm{s}$ incorporates the tractions t_s due to the driving forces. The data exchange has to be done only once for a given model, as $\boldsymbol{M}_\mathrm{s}$ and $\boldsymbol{K}_\mathrm{s}$ are frequency independent. In this paper, hysteretic damping is considered with the damping matrix

$$\boldsymbol{D}_\mathrm{s} = \eta\, \boldsymbol{K}_\mathrm{s}\,, \tag{15}$$

and the damping parameter η. Typically, shell elements with translational and rotational degrees of freedom are applied for thin structures. Thus, each node generally has six degrees of freedom, which are $\{u_x,u_y,u_z,\theta_x,\theta_y,\theta_z\}$. In the frequency domain, the resulting FE system reads

$$\underbrace{\left(-\omega^2 \boldsymbol{M}_\mathrm{s} - \mathrm{i}\omega \boldsymbol{D}_\mathrm{s} + \boldsymbol{K}_\mathrm{s}\right)}_{\boldsymbol{K}_\mathrm{FE}} \boldsymbol{u} = \boldsymbol{f}_\mathrm{s} - \boldsymbol{C}_\mathrm{FE}\, \boldsymbol{p}\,, \tag{16}$$

where a coupling matrix $\boldsymbol{C}_\mathrm{FE}$ is introduced. It converts the nodal pressure values to the force components of the structure. It is assembled from the element matrices

$$\boldsymbol{C}_\mathrm{FE}^k = \int_{\tau_k} \boldsymbol{N}_u^\mathrm{T}\, \boldsymbol{N}_p\, \boldsymbol{n}_x \,\mathrm{d}s_x\,, \tag{17}$$

where $\boldsymbol{N}_u$ and $\boldsymbol{N}_p$ contain the shape functions. Here, a lumped force loading is applied, which neglects moments. Please note, that not all structural nodes are in contact with the water. Thus, $\boldsymbol{C}_\mathrm{FE}$ has zero entries for the corresponding degrees of freedom.

4 Coupled Problem

Coupling the BE equations (6) and (8) with the FE equation (16) yields the linear block system of equations

$$\underbrace{\begin{pmatrix} \boldsymbol{K}_\mathrm{FE} & \boldsymbol{C}_\mathrm{FE} \\ \boldsymbol{C}_\mathrm{BE}\boldsymbol{T}_q & \boldsymbol{K}_\mathrm{BE} \end{pmatrix}}_{\boldsymbol{K}} \underbrace{\begin{pmatrix} \boldsymbol{u} \\ \boldsymbol{p} \end{pmatrix}}_{\boldsymbol{x}} = \underbrace{\begin{pmatrix} \boldsymbol{f}_\mathrm{s} \\ 0 \end{pmatrix}}_{\boldsymbol{b}}\,. \tag{18}$$

As outlined in [6], elimination of $\boldsymbol{u}$ yields a Schur complement representation of the coupled system

$$\underbrace{\left(\boldsymbol{K}_\mathrm{BE} - \boldsymbol{C}_\mathrm{BE}\boldsymbol{T}_q\, \boldsymbol{K}_\mathrm{FE}^{-1} \boldsymbol{C}_\mathrm{FE}\right)}_{\boldsymbol{S}} \boldsymbol{p} = -\boldsymbol{C}_\mathrm{BE}\boldsymbol{T}_q\, \boldsymbol{K}_\mathrm{FE}^{-1} \boldsymbol{f}_\mathrm{s}\,, \tag{19}$$

where $\boldsymbol{S}$ denotes the Schur complement.

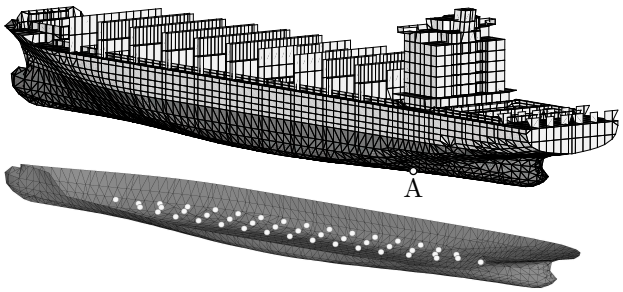

Figure 3: Discretized model of the container-vessel "Zim" (top). The wet boundary elements are highlighted in dark gray. Light spots indicate the position of the used monopole sources (bottom).

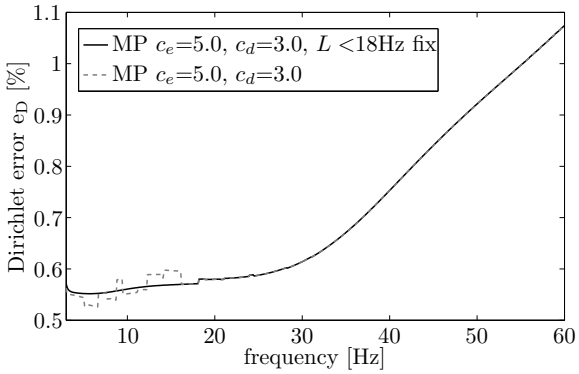

Figure 4: Dirichlet errors for monopole problem.

4.1 Iterative Solution Strategy

As discussed above, the FMM helps to efficiently compute the BE matrix–vector products. It is especially well suited in combination with an iterative solver. In the following, a preconditioned GMRES is applied to solve the Schur complement system (19). In every iteration step, the effect of the inverse of the FE matrix on a vector has to be computed. Since the condition number of the FE matrix is high, a direct factorization based LU solver is applied for this purpose. This has the advantage, that the factorization has to be computed only once and can then be reused during the solution process.

The GMRES solver is preconditioned with an ILU or scaling preconditioner, working on the near-field matrix of $\boldsymbol{K}_{\mathrm{BE}}$. Thus, this preconditioner neglects the feedback of the acoustic pressure onto the structure.

5 Numerical Example

As model problem, the container vessel "Zim" which is depicted in Fig. 3 is investigated. It has a length of 253 m, a width of 32.2 m and a draft of 10.8 m. The discretized model consists of approximately 36,000 structural degrees of freedom and approximately 1,500 wet nodes with pressure degrees of freedom. The nodes of the boundary elements coincide with the nodes of the finite elements. The structure is driven by 110 semi-artificial forces, which reflects the excitation of the structure by the screw.

5.1 Simulation Error of the BE Part

First, the pure acoustic problem is investigated. An artificial acoustic field is generated by using monopole sources as depicted in Fig.3 (bottom). To satisfy the pressure-free boundary condition on the water surface, all sources are mirrored on the half-space plane and the strengths of the mirrored sources are multiplied by -1. The corresponding flux field is used as Neumann boundary condition on Γ_{I}. Now the BEM is used to compute the pressure at all nodes. The pressure is then compared with the corresponding pressure of the analytical field. Therefor, the Dirichlet error

$$\mathrm{e_D} = \frac{\|\boldsymbol{p}_{\mathrm{BEM}} - \boldsymbol{p}_{\mathrm{analyt.}}\|_2}{\|\boldsymbol{p}_{\mathrm{analyt.}}\|_2} \qquad (20)$$

is analyzed. The errors are visualized in Fig. 4 for FMM with different expansion lengths. For the FMM, the near-field parameter in (9) is chosen as $c_d = 3$. The expansion lengths of the multipole method are computed by (13) with $c_e = 5$. The use of the semi-empirical rule (13) leads to error jumps in the low frequency regime. This is because the rule is optimized for a ratio of 6 to 10 elements per wavelength. Here, the ratio is 28 at a frequency of 20 Hz. The jumps are avoided by computing the expansion length using (13), but fixing the frequency to 18 Hz for all frequencies below 18 Hz. This leads to a slightly increased expansion length for small frequencies. Obviously, the additional errors by the FMM is negligible compared to the discretization error.

5.2 Results of the Coupled Approach

Now the fully coupled system (19) is investigated. For the FMM, the same parameters as discussed in the last section are applied. Figure 5 shows the acoustic pressure at node A (cf. Fig3). As comparison, also the solution of the one-way coupled problem is plotted. One-way coupling means, that $\boldsymbol{C}_{\mathrm{FE}}$ in (19) is set to zero. Thus, the feedback of the acoustic pressure is neglected and the structural and acoustical problems are solved consecutively. As can clearly be seen, the results of the strong coupling scheme differ significantly from the one of the one-way coupling. Obviously, the feedback of the pressure cannot be neglected and a fully coupled simulation is unavoidable.

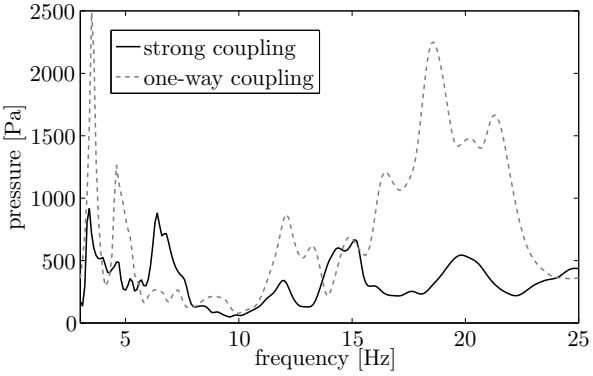

Figure 5: Pressure at node A of the vessel.

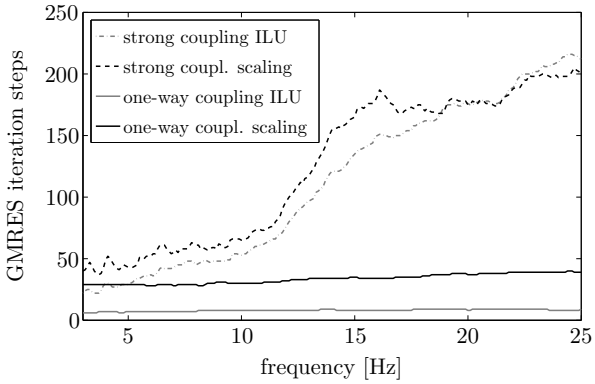

Figure 6: GMRES iteration steps, full coupling versus one way coupling for different preconditioners.

5.3 Efficiency

The number of iteration steps of the GMRES has a direct influence on the simulation time. To improve convergence, an ILU or scaling preconditioner is applied to the near-field matrix of $\boldsymbol{K}_{\mathrm{BE}}$. Figure 6 shows the number of iteration steps for an accuracy of 1e-6. In case of the one-way coupling, convergence is almost independent of the frequency and optimal for a ILU preconditioner. Even a simple scaling works well. For the strong coupling, the number of iteration steps increases. This is as one would expect, since the one-way coupled system is used for preconditioning. Here, the ILU works hardly better than the scaling preconditioner. In this case, the convergence could be further improved by incorporating the second part of the Schur complement into the preconditioning.

A significant portion of the computation time is needed for setting up the near-field matrices of the FMM. For the presented model, 24.7% of the computation time is spent for the mirrored part. This is a rather small model for the FMM. The far-field compression works better for larger models. To demonstrate this, the boundary elements are simply split into smaller elements with half of the sidelength, leading to 5,891 wet nodes. Now, only 10.8% are spent for the mirrored part. Another refinement leads to 23,213 nodes and a portion of 6.4%. The efficiency is better for larger models, since the number of elements in the near-field clusters within the mirrored part is smaller compared to the overall number of elements.

Besides the near-field integration, also the expense of a single iteration step is of importance. Here, mainly the far-field of the FMM has a significant contribution. The mirrored part leads to an increase of applied translation operators of 119% for the original model and of 47% and 18% for the refined ones, respectively. But this behavior cannot be seen for the total computation time of the far-field, which increases by approximately 30% for all models. The upward pass is only slightly more expensive, because of the additionally applied translations. Most of the time is spent with the computation of the near-field signature, which remains unchanged. The downward pass, which is generally cheaper than the upward one, is doubled, since all operations have to be done for the original and the mirrored part.

6 Conclusion

In this paper, a strong coupling scheme between the fast multipole BEM and the FEM is presented for the simulation of fluid-structure coupled problems. For the investigation of ship-like structures, the free water surface has to be incorporated into the BEM formulation of the fluid part. An efficient approach is the use of a special half-space fundamental solution. This avoids the discretization of the free water surface. To overcome the drawback of fully populated matrices in case of standard BEM implementations, the fast multipole method is applied. The realization of the half-space fundamental solution involves some modifications of the standard multipole procedure. A simple and efficient implementation is obtained by a mirror technique, which duplicates the original model. Numerical tests show, that the additional cost for the modified fundamental solution is smaller than 30% for large models.

Acknowledgments

This research was financially supported by the German Research Foundation (DFG) under the transfer project SFB404/T3. The authors acknowledge valuable contributions of Prof. Olaf Steinbach and Dr. Günther Of of the Technical University of Graz within this transfer project.

References

[1] A. Seybert, B. Soenarko, "Radiation and scattering of acoustic waves from bodies of arbitrary shape in a three-dimensionla half space", *Transactions of the ASME 110*,112–117, (1988)

[2] V. Rokhlin, "Rapid solution of integral equations of classical potential theory", *J. Comput. Phys. 60*, 187–207, (1985)

[3] R. Coifman, V. Rokhlin, S. Wandzura, "The fast mulipole method for the wave equation: A pedestrian prescription", *IEEE Antenn. Progag. M. 35*, 7–12, (1993)

[4] M. Epton, B. Dembart, "Multipole translation theory for the tree-dimensional Laplace and Helmholtz equation", *SIAM J. Sci. Comput. 16*, 865–897, (1995)

[5] S. Amini, PJ. Harris, DT. Wilton, "Coupled Boundary and Finite Element Methods for the Solution of the Dynamic Fluid-Structure Interaction Problem, Lecture Note in Engineering Vol.77", *Ed. CA. Brebbia and SA. Orszag, Springer-Verlag London*, (1992)

[6] D. Brunner, M. Junge, L. Gaul, "A comparison of FE-BE coupling schemes for large scale problems with fluid-structure interaction", *Int. J. Numer. Eng.*, submitted for publication